Voltage-Induced Cholesteric Structure-Transformation in Thin Layers

Paul R. Gerber

Central Research Units, F. HOFFMANN-LA ROCHE & CO., Limited Company, Basel Switzerland

Z. Naturforsch. **36a**, 718–726 (1981); received April 10, 1981

Measurements of various threshold voltages which occur in thin layers of cholesteric liquid crystals with positive dielectric anisotropy under homeotropic wall-alignment conditions are presented. Characteristic times are determined for some of the structure-changing processes which take place under application of electric-field changes. The measurements have been performed for various pitch-to-thickness ratios, and are expressed in empirical formulae.

1. Introduction

Liquid crystal displays of the guest-host type have found a lively interest in recent years, as better dye molecules become available [1 – 3]. Advantages are the good angular dependence of the contrast and the high brightness. This is especially the case in displays utilizing the field-induced cholesteric to nematic phase change effect [2, 4 – 6], since no polarizers are needed. This effect can also be utilized in light-scattering displays [6, 7]. Due to the complicated deformations encountered in cholesteric liquid crystals when subjected to restricted geometric and alignment conditions the physics of such display cells is rather complex [8 – 13]. It is the purpose of this paper to study quantitatively some aspects of the phase change transformations in planar cells. We have restricted ourselves to the case of homeotropic wall alignment which appears to be most interesting for practical applications.

Under these conditions several textures are important. Without applied voltage across the cell the so called *scroll texture* is seen, which shows a spatial modulation in the cell plane with the appearance of an array of spiraling structures (for a picture see [9], Figure 4). However, this structure still has essentially the properties of the Grandjean texture which is commonly observed under parallel wall alignment conditions. But a planar adaption to the unfavourable homeotropic boundary conditions seems unstable against the observed distortion.

Reprint requests to Dr. P. Gerber, Central Research Units, F. Hoffmann-La Roche & Co., Limited Company, 4002 Basel, Schweiz.

For substances with positive dielectric anisotropy as used in our experiments application of a small voltage across the cell leads to a rather continuous transformation to the well known *fingerprint texture* in which the cholesteric helix axis lies in the cell plane. The analogous transition in planar orienting samples takes place via a biperiodic grid-texture [14], which may be viewed in analogy to the spatial modulation of the scroll texture.

Higher applied voltages eventually lead to a *complete homeotropic alignment.*

Occasionally one can observe at intermediate voltages arrangements of spherulitic structures [15, 16], sometimes called bubbles, which have no analogue in the parallel-alignment case.

Upon lowering the voltage in the homeotropic state it may occur that domains of the fingerprint-structure start to grow by nucleation. However, if suitable nucleation centers are absent or if the voltage is lowered at a fast rate, the homeotropic state transforms directly into a *planar conical state.* As in the Grandjean state a helix with axis perpendicular to the substrate develops but the director and substrate plane are at a (nonzero) angle which varies with distance from the substrates. This transient planar state may subsequently decay directly into the scroll texture or into a fingerprint like pattern depending on applied voltage and thickness to pitch ratio.

The alternate routes of structure transformation observed upon reducing the voltage illustrates the importance of hysteresis effects in the cholesteric-nematic phase change transformation. Most structures have regions of rather long living metastability, and in addition the irregular growth of some pat-

0340-4811 / 81 / 0700-0718 $ 01.00/0. — Please order a reprint rather than making your own copy.

terns leads to slow subsequent relaxation processes by migration of disclination lines.

The aim of the present work is to determine the stability conditions for the various structures and to study some dynamical aspects of the transformation processes.

2. Experimental

We have made all measurements with the nematic mixture RO-TN-605 from Hoffmann-La Roche exhibiting nematic order over a large temperature range ($\sim -30\,^{\circ}\mathrm{C}$ to $96\,^{\circ}\mathrm{C}$). The measurements were performed at $40\,^{\circ}\mathrm{C}$. At this temperature the following physical properties were determined:

Dielectric constants: $\varepsilon_{\parallel} = 17.55$, $\varepsilon_{\perp} = 5.4$;

Elastic constants: $k_{11} = 10.9 \cdot 10^{-12}\,\mathrm{N}$, $k_{22} = 6.2 \cdot 10^{-12}\,\mathrm{N}$, $k_{33} = 17.1 \cdot 10^{-12}\,\mathrm{N}$;

Rotational viscosity: $\gamma_1 = 1.162\,\mathrm{Poise}$. (2.1)

In order to induce a cholesteric phase we have added small amounts of 4-Cyano-4′-(2-methylbutyl)biphenyl (CB15 from BDH) which has a twisting power in RO-TN-605 of

$$1/c\,P = 7.14 \cdot 10^{-2}\,[\mu\mathrm{m} \cdot \mathrm{wt}\%]^{-1}, \qquad (2.2)$$

where P is the pitch of the cholesteric structure and c the concentration of CB15 in weight percent.

The substances were filled into wedge-shaped cells with two different spacers of 10 and 50 microns, separated by about 25 mm. The glass surfaces were coated with silanes so as to induce homeotropic alignment near the walls. Most observations were made with a polarizing microscope while the cell was driven by an alternating voltage of 1.6 kHz. Ohmic conductivity in the cells was negligible. Most measurements were made on two such wedge-cells. Cell 1 was filled with a 1%-CB15-solution of a pitch of 14 microns, cell 2 contained a 2%-solution (pitch = 7 μm).

3. Stability Regimes of Cholesteric Textures

3.1. Scroll Texture

A well aged cell in zero voltage shows the scroll texture, provided the pitch-to-thickness ratio is not too large. Although a pronounced spatial modulation is seen, this structure appears to be essentially a Grandjean type texture, as shown by capacitance (C) measurements, which indicate that the average orientation of the director of the liquid crystal is nearly parallel to the substrate. In particular we have measured $C/C_{\parallel} = 0.37$, 0.38, and 0.43 for $P/d =$ 0.16, 0.23, and 0.47 respectively ($C_{\parallel}$ is the capacitance corresponding to complete homeotropic alignment and d is the cell thickness).

However, in the limit $P/d \to 0$ this sequence appears to reach a value of $C/C_{\parallel} \approx 0.34$ which lies somewhat above $\varepsilon_{\perp}/\varepsilon_{\parallel} = 0.308$. This may be an indication that the scroll texture exhibits, apart from distorted boundary zones, a helical axis which is somewhat tilted with respect to the substrate normal. For non-zero values of the ratio P/d this "tilt" may, however, have oscillatory components in P/d. In this context we would like to mention that we observed in wedge-shaped cells a periodicity in the appearance of the scroll texture with a period given roughly by the distance over which the cell thickness changed by half a pitch.

When the applied voltage increases the helical axis rotates in a direction parallel to the substrate and the well known fingerprint texture starts to developed. This is a process which takes place in a finite voltage interval and which is very slow. Observation of the capacitance of the cell or of the light transmission in a polarizing microscope as a function of the applied voltage shows a well pronounced step [13, 17], the position of which shifts towards smaller voltage values when the sweeping speed decreases.

This behaviour is illustrated in Fig. 1 where the capacitance of a cell is shown as a function of the applied voltage for different sweeping rates of increasing and decreasing voltage. The simple description in terms of a helical axis is, of course, only a qualitative picture of the rather complicated director pattern found in these structures, but it does give a rough characterization of the capacitance measurements.

Figure 2 shows among other data, the voltages V_{tilt} multiplied by P/d at which the optically observed steps occurred for a slow sweeping speed of 85 mV/min (Graph "tilt"). These observations were made at different locations in the two cells, 1 and 2. For small values of P/d the process seems to be essentially voltage-controlled, although it is not quite clear whether and how $V_{\mathrm{tilt}}(P/d)$ reaches zero for $P/d \to 0$. An upper limit is given by $P/d \approx 0.73$, above which the scroll texture ceases to show up.

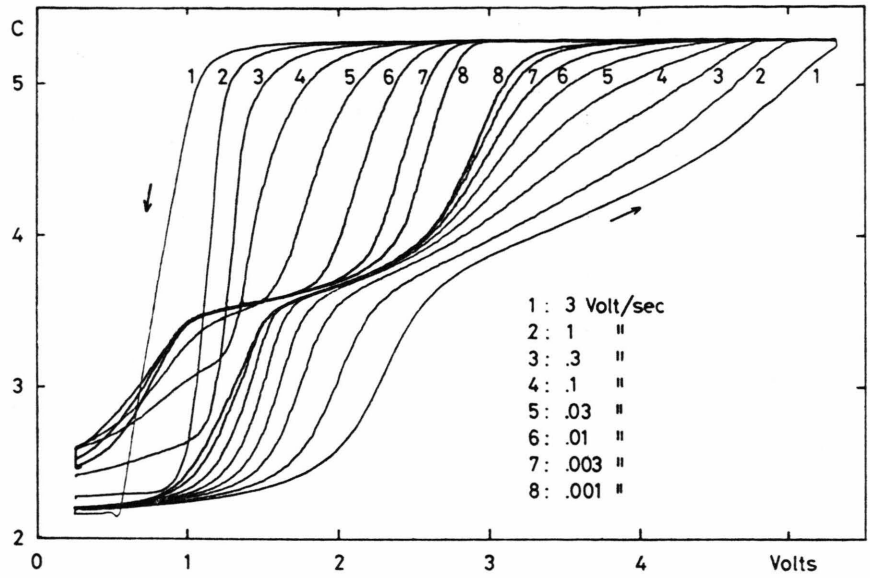

Fig. 1. Capacity of a parallel cell as a function of applied voltage. Full cycles are recorded with different sweeping rates. Two pronounced steps are visible. At voltages below the first step the liquid crystal is essentially in a planar texture, although a spatial modulation can be observed (scroll texture). During the first step the helix axis turns in a direction parallel to the substrate, leading to a fingerprint texture. In the second step the totally homeotropic state is reached. In the reverse sweeping direction the processes are reversed but the rearrangement in the fingerprint and scroll textures are so slow that a considerable hysteresis is seen even at very slow sweeping rates. For fast down-sweeping the direct formation of the planar state is observed giving a very steep step. The parameters were $P = 4.7\ \mu$, $d = 10\ \mu$.

3.2. *Fingerprint Texture*

For voltages larger than V_{tilt} the well known fingerprint texture is seen and remains unchanged apart from some pitch adjustment up to a voltage $V_{\text{ch,n}}$, above which the nematic structure is stable. This voltage $a_{\text{ch,n}}$ is easily observed in wedge-shaped cells where a pronounced borderline between homeotropically aligned nematic and fingerprint texture is observed after keeping the applied voltage constant for a couple of minutes. The measured values $V_{\text{ch,n}}(P/d)$ are shown versus P/d in Fig. 2 (Graph "ch, n"). The differences between the two cells 1 and 2 are within the limits of accuracy with which the cell geometry could be determined. However, apart from geometry uncertainties one can imagine differences between the two cells occurring, due to the influence of imperfect strong anchoring at the surfaces which would spoil the scaling laws. For large cell thickness the results can be fitted by an asymptotic expression

$$V_{\text{ch,n}} \frac{P}{d} = V_0 - V_1 \frac{P}{d} + \dots . \tag{3.1}$$

The measurements yielded the coefficients

$$V_0 = \begin{cases} 2.42\ \text{V}, & \text{cell 1}, \\ 2.45\ \text{V}, & \text{cell 2}, \end{cases} \tag{3.2}$$

and

$$V_1 = \begin{cases} 1.99\ \text{V}, & \text{cell 1}, \\ 1.78\ \text{V}, & \text{cell 2}. \end{cases} \tag{3.3}$$

The value of V_0 should coincide with the threshold voltage for the cholesteric-nematic transition as calculated by de Gennes [4].

$$\lim_{d\to\infty} \left(V_{\text{ch,n}} \frac{P}{d} \right) = \pi^2 \sqrt{\frac{k_{22}}{\Delta\varepsilon\, \varepsilon_0}} = 2.37\ \text{Volt}. \tag{3.4}$$

The last value was obtained from the data (2.1) and agrees with V_0 well within the limits of experimental uncertainties.

Above a critical value $(P/d)_c = 0.98$ (cell 1) a homeotropic nematic order is favoured over the fingerprint texture in zero applied voltage. Near this value the critical voltage $V_{\text{ch,n}}$ was found to obey the asymptotic expression

$$\left(V_{\text{ch,n}} \frac{P}{d} \right) = V_2 \sqrt{\left(\frac{P}{d} \right)_c - \frac{P}{d}}\ . \tag{3.5}$$

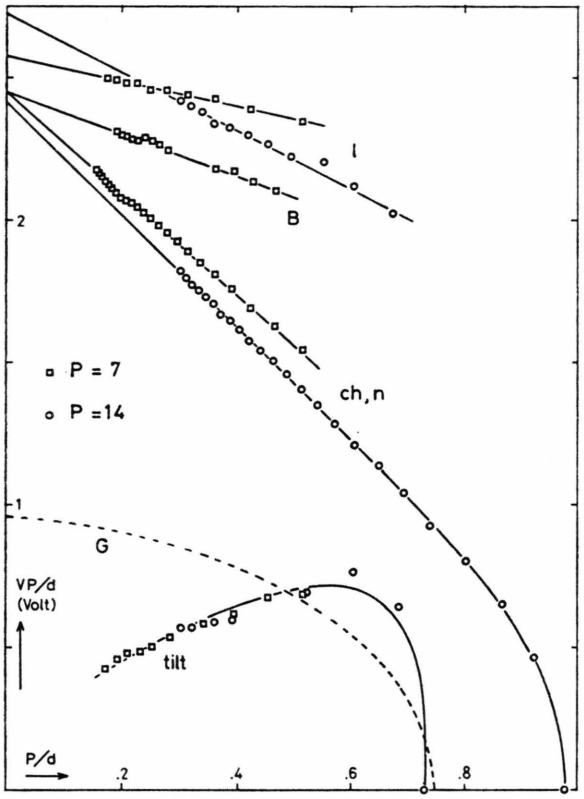

Fig. 2. Threshold voltages multiplied by P/d versus P/d for various structure transformations: Tilting of the scroll texture (tilt), cholesteric-nematic threshold (ch, n), stability limit of bubbles (B) and of cholesteric lines (l). Measurements were taken in cell 1 ($P = 14$ μ) and cell 2 ($P = 7$ μ). The dashed line G for the threshold voltage V_G is drawn for comparison with $V_{ch,n}$ or V_l in order to demonstrate the large hysteresis effects. Measured points for V_G are shown in Figure 3.

For cell 1, in which the critical thickness could be observed, we obtained a value $V_2 = 1.92$ V.

For voltages above the stability limit of cholesteric spherulites which are considered in the next section we observed an additional limit of metastability related to the fingerprint texture, namely the one for the existence of single cholesteric lines. These lines, which have been described as 360°-walls in a nematic state [10], were observed when the fingerprint texture was about to disappear. Normally most cholesteric lines ended somewhere in a "half bubble" (for pictures see Ref. [10]). When the voltage was raised above $V_{ch,n}$ these ends retreated and after some time the cholesteric lines of finite length usually had contracted to cholesteric bubbles which remained present unless the voltage was above V_B (see Section 3.3). Of course, one can imagine having cholesteric lines both ends of which are tied to some surface structure or impurity and which are hence prohibited from shrinking. However, when the applied voltage was raised high enough, the lines broke spontaneously and thus disappeared. We have measured the threshold voltage V_l above which the lines break. But since most of the observable lines had retreating ends, breaking had to occur before the lines disappeared by shrinking. For this reason the measured voltages V_l may be somewhat high and subjected to systematic errors. The obtained threshold voltages for breaking are also plotted in Fig. 2 (Graphs "l"). They, too, show a linear asymptotic behaviour for small P/d. However, the limiting values for P/d as well as the slopes differ appreciably for the two cells. This lack of scaling may well be due to the above-mentioned systematic uncertainties. In addition one has to keep in mind that for metastable structures the question of "stability" always involves a time scale. From a general point of view our measured values for V_l may be subject to some arbitrariness. However, for practical application V_l is important because it indicates the limit above which a cholesteric fingerprint texture can be forced to disappear speedily due to the generation of retreating line ends.

3.3. *Cholesteric Bubbles*

For voltages above $V_{ch,n}$ we have sometimes observed cholesteric bubbles [15, 16]. They could not always be systematically generated, but in cell 2 we observed enough of them to enable us to perform a systematic measurement of the voltage interval within which they did not disappear. It was found that the bubbles exist only below a threshold voltage V_B which depended on P/d. This dependence is also plotted in Fig. 2 (Graph "B"). Here, too, the measurements extended over a sufficient range of values of P/d to enable us to derive an asymptotic law for small values of the form

$$V_B \frac{P}{d} = \overline{V}_0 - V_3 \frac{P}{d} + \dots . \tag{3.6}$$

Within the limits of accuracy the voltage $\overline{V}_0$ agrees with the corresponding value V_0 of Eq. (3.1) for the cholesteric-nematic transition. However, the slope

$$V_3 = 0.74 \text{ Volt, cell 2} \tag{3.7}$$

is smaller than V_1 by more than a factor of two.

We have not been able to make reliable measurements for values of P/d above 0.5, although the occurrence of bubbles was observed in cell 1 on rare occasions.

3.4. Planar States

As mentioned in the Introduction the deformation pattern follows often a different route when the applied voltage is lowered. This gives rise to a pronounced hysteresis effect. Below the voltage $V_{\mathrm{ch,n}}$ cholesteric lines in principle can grow and eventually form an extended fingerprint texture. However, this is a fairly slow process for voltages near $V_{\mathrm{ch\text{-}n}}$ and, moreover, requires nucleation of lines from defects present in the cell. On the other hand when the voltage is lowered fast enough this process is no longer important, but one encounters below a threshold V_{G} a process which has been discussed by Greubel [17]. The liquid crystal develops a planar texture with a helical axis but shows a conical helical structure with variable cone-angle. The threshold voltage obeys [17] the equation

$$\left(V_{\mathrm{G}}\frac{P}{d}\right)^2=\frac{\pi^2}{\varepsilon\Delta\varepsilon}\left[\frac{4\,k_{22}^2}{k_{33}}-k_{33}\left(\frac{P}{d}\right)^2\right]. \quad (3.8)$$

We have measured V_{G} in the wedge-shaped cells by starting from a homeotropic texture with $V>V_{\mathrm{ch\text{-}n}}$. After suddenly reducing the voltage we observed a borderline at a locus of constant cell thickness. In the region of higher thickness one could see the uniform appearance of the planar texture while in the thinner regions a fingerprint texture started to grow. The voltage at the cell was then interpreted as V_{G}, corresponding to the cell thickness at the borderline. Figure 3 shows a plot of the measured values $(V_{\mathrm{G}}(P/d))^2$ versus $(P/d)^2$. Each cell gives a reasonably linear graph which agrees fairly well with the theoretical curve obtained from Eq. (2.11) together with the measured material parameters (2.1). In appreciating the agreement one has to keep in mind that P/d enters squared in both coordinates thus augmenting all uncertainties in the cell geometry. In addition the uncertainties in the elastic constants which are about 4% show up quite distinctly at the intersections with the axes while the slope is less influenced by them. The planar texture which first develops deforms then into the scroll texture. For $P/d \lesssim 0.29$ the scroll texture does not appear directly but a fingerprint-like intermediate structure, with many disclination lines, follows first. These lines disappear slowly and the structure develops the scroll appearance. This intermediate structure may be generated by the undulation instability [18] which stems from the fact that in the process of forming the planar structure from the homeotropic one the wrong pitch of size $P(k_{33}/k_{22})$ first develops. Thus it seems that for $P/d>0.29$ the pitch can still adjust to the correct value by changing the number of turns within the planar structure while for $P/d<0.29$ the undulation destroys the planar texture. It is to be expected that this critical value of P/d depends strongly on k_{33}/k_{22} and vanishes for $k_{33}=k_{22}$.

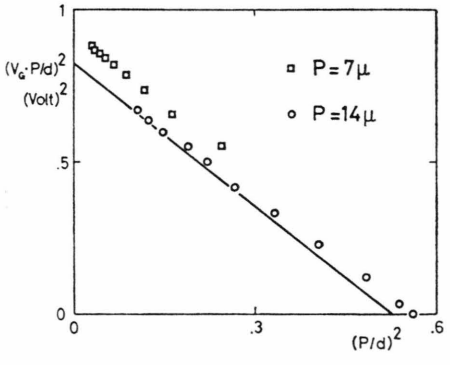

Fig. 3. Threshold voltage V_{G} for the transition homeotropic to conical helix. Plotted is $(V_{\mathrm{G}}P/d)^2$ versus $(P/d)^2$ which is expected to give a linear behaviour. The straight line is calculated from Eq. (3.8) with the data (2.1).

4. Dynamical Aspects of Cholesteric Texture Transformations

In the cycle of texture transformations described in the previous sections there are a few processes the dynamics of which seemed worth an investigation. The corresponding measurements have been made with the cell 2. The structures were monitored by observing the light transmitted through the sample in a polarizing microscope with polarizer and analyser crossed.

4.1. Transitions from the Homeotropic State

First we consider the processes that take place when an applied voltage, sufficiently high to keep the liquid crystal in a nematic state, is reduced suddenly to a voltage $V<V_{\mathrm{G}}$. In this case a conical helix first appears. The time scale τ_{G} on which this structure develops is dependent on the remaining applied voltage. Figure 4 shows a typical plot of

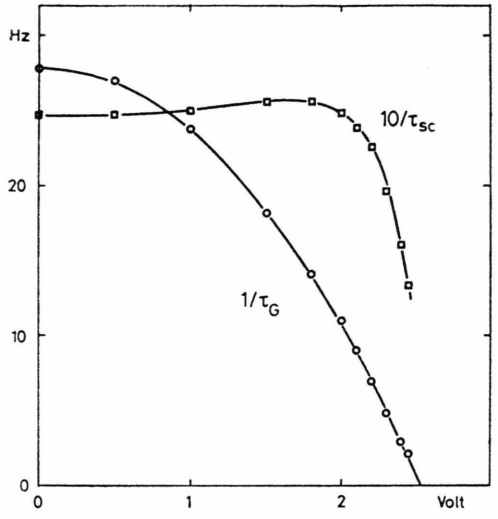

Fig. 4. Rate of appearance of the conical helix τ_G^{-1} after suddenly reducing the applied voltage from 12.4 V — which corresponds to homeotropic alignment — to the value shown on the abscissa. Also shown is the rate τ_{sc}^{-1} of formation of the scroll texture which follows the conical spiral structure. The parameters are $P=7\ \mu$, $d=20.5\ \mu$, $\bar{V}_G=2.53$ V. Above 1.75 V a tilted structure is more stable than the scroll texture.

τ_G^{-1} versus applied voltage. This reciprocal time starts at some saturation value $\tau_{G,0}^{-1}$ with zero voltage remaining across the cell and decreases towards zero when the voltage approaches a limiting value $\bar{V}_G$ which agrees well with the threshold voltage V_G. The reciprocal characteristic time may asymptotically (as $V \uparrow \bar{V}_G$) be described by a linear law

$$\tau_d/\tau_G \approx a(\bar{V}_G - V), \quad V \uparrow \bar{V}_G, \tag{4.1}$$

where we have introduced the characteristic thickness dependent time

$$\tau_d = d^2 \gamma_1/k_{11}. \tag{4.2}$$

For voltages very close to $\bar{V}_G$ the development of the planar structure becomes dominated by the growth of the fingerprint texture which starts by nucleation at the imperfections present in the cell. This leads to a rounding of the curve (4.1) near the voltage $\bar{V}_G$.

Figure 5 shows a plot of the coefficient a versus P/d as determined from measurements in cell 2. This quantity saturates below $(P/d) \approx 0.3$ towards a value of $a \approx 115\ \text{Volt}^{-1}$ while for large pitch-values a decreases sharply. Towards the limiting value $(P/d \approx 0.75)$ for which the conical helix can just develop, the coefficient a appears to decrease towards zero faster than linearly.

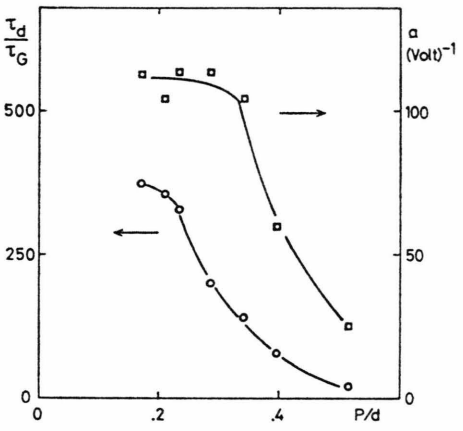

Fig. 5. Limiting value of τ_G^{-1} for zero voltage remaining at the cell, in units of τ_d^{-1} (4.2) and slope a (4.1) versus P/d.

The normalized speed $\tau_d/\gamma_G(V=0)$ with which the conical helix develops in zero applied field is shown also in Figure 5. It seems to reach a limiting value only for $P/d=0.2$, while for large values of P/d an extremely steep decrease is seen.

The conical helix pattern keeps developing directly into the scroll texture as long as $P/d>0.29$. The time scale τ_{sc} on which this process takes place is only slightly dependent on the remaining voltage at the cell as long as it has a value below V_{tilt} (see Figure 4). The reduced rate τ_d/τ_{sc} increases remarkably steeply with decreasing P/d ($\tau_d/\tau_{sc}=3.2$ and 8.9 for $P/d=0.51$ and 0.34, respectively).

4.2. *Transformation to the Homeotropic State*

When generating the homeotropic state it is important whether the applied voltage V lies above or below V_1, the critical voltage for line breaking. We restrict ourselves to the case $V>V_1$ which due to the breaking of cholesteric lines is less susceptible to the domain structure of the fingerprint texture we start from. In these measurements the voltage was first kept slightly below $V_{ch,n}$. After a sudden raise to a value above V_1 the disappearance of the fingerprint texture was monitored.

Figure 6 shows an example of these measurements. We plotted $(\tau_h V)^{-1}$ versus reciprocal applied voltage V^{-1}, where τ_h is the characteristic time of disappearance of the fingerprint texture. From this graph it appears that $(\tau_h V)^{-1}$ reaches a finite limit for in-

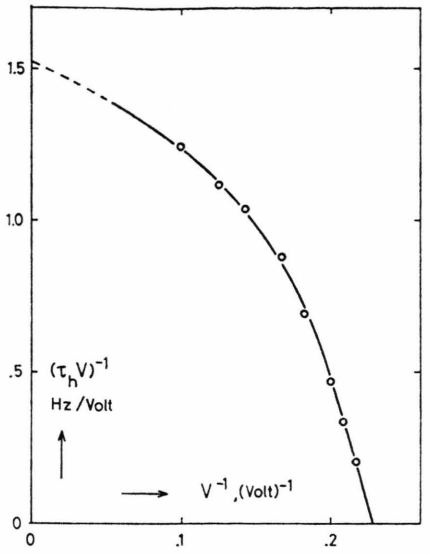

Fig. 6. $(\tau_h V)^{-1}$ versus applied voltage V. The characteristic time τ_h measures the appearance of the homeotropic texture after the voltage has been raised to a value V from a value of 2.9 V at which a stable fingerprint texture was present. Other parameters are: $P=7\ \mu$, $d=13.6\ \mu$. The threshold voltage V_1 for stable cholesteric lines was 4.5 V.

creasing voltage V, while a steep decrease takes place as the voltage is lowered towards the critical voltage of stable cholesteric lines V_1. Table 1 shows the limiting values of a disappearance rate

$$b=\tau_d/(\tau_h V), \tag{4.3}$$

for the limit $V\to\infty$. The values were obtained by rather extended extrapolations of b-versus-V^{-1} plots to the axis $V^{-1}=0$. It seems that the limiting value of b reaches a constant value of about 1.6 Volt^{-1} for $P\gg d$, and increases markedly for $P>d/3$.

When the voltage applied after the step approaches V_1, b decreases steeply as seen in Figure 6. The data suggest a linear dependence of b on V^{-1} near the axis $b=0$. However, it appears possible that a steeper decrease with round-off effects simulates an asymptotic linear law. Nevertheless we have fitted the data with a form

$$b\approx c(\overline{V}_1^{-1}-V^{-1}),\quad V\searrow V_1. \tag{4.4}$$

The values of $\overline{V}_1$ lie slightly above the values of V_1 which mark the stability limit of cholesteric lines against spontaneous breaking as described in section 3.2. The coefficients c which have values around about 50 are shown in Table 1.

Previous measurements [19] using rather high fields indicated the existence of a finite limit for

Table 1. Extrapolated limiting values for $V\to\infty$ of the disappearance rate (4.3) of the fingerprint texture after application of a voltage step for different values of P/d. Also shown is the coefficient c in (4.4) describing the limiting behaviour for $V\to\overline{V}_1$.

P/d	$\tau_d/(\tau_h V)$	c
0.233	1.98	33.7
0.341	2.25	43.2
0.515	3.00	65.8

τV^2 as $V\to\infty$. However, for the voltage range considered in the present work a limiting dependence $\tau\sim V^{-1}$ for $V\to\infty$ seems to be more appropriate as illustrated in Figure 6.

5. Conclusions

There are few theoretical considerations in the literature to which the present measurement may be related. Firstly, the threshold voltage for the cholesteric-nematic phase change transformation [4] (Eq. (2.7)) was obtained by extrapolation. Furthermore, the asymptotic behaviour of $V_{ch,n}$, as expressed in the coefficient V_1 (3.3), contains information about the energy stored in the transition region which mediates between the uniform homeotropic order near the substrates and the cholesteric director pattern in the middle of the cell. The empirical linear behaviour in d^{-1}, as measured and expressed in (3.1), must probably be corrected by logarithmic contributions originating from pitch dilatations in the presence of the electric field. However, such corrections are beyond the measuring accuracy.

Press and Arrot [10] have presented very instructive computer simulations which explain the topology of the director pattern in the transition region. For a quantitative comparison with our experiments their calculations are not suited because they apply the one constant approximation $k_{11}=k_{22}=k_{33}$ which is inadequate for our case (see (2.1)). Previous calculations [20] make, in addition, ad hoc assumptions about the director pattern.

Calculations dealing with the cholesteric-bubble-structure [21] are still on the level of an assumed director pattern with circular disclination lines near the surfaces. Stieb [11] has extended the topological results of Press and Arrott [9] to obtain proposals for the bubble structure. However, these proposals have not been put on a computer to allow for quantitative comparison with our measured values of V_B.

The metastability threshold of lines V_1 appears to have not been treated theoretically. Although Press and Arrott [10] mention a collapse to the homeotropic configuration it is questionable whether a calculation restricted to two spacial dimensions can explain this phenomenon.

The picture emerging from Press and Arrotts calculations suggests that what we called the tilting of the helical axis is not a threshold effect but more of a steep but gradual change (see e. g. $\theta_{\min,\max}$ in Fig. 12 of Ref. [9]). This is consistent with the rather broad transition region found in the tilting process. However, it seems probable to us that V_{tilt} of Fig. 2 may be connected with a rapid change of $\theta_{\min,\max}$ of Ref. [9] as a function of applied voltage.

A further point concerns the relative stability of homeotropic, planar conical and periodic structures in zero field. While Press and Arrott find that below a critical thick ness $d_c = \frac{1}{2} P$, at which the planar state ceases to exist, a periodic structure is also absent. On the other hand, our measurements indicate a critical value $(P/d)_{\text{pl}} = 0.76$ above which the planar structure does not develop from the homeotropic state (see Figure 3). This compares reasonably well with the value $2\,k_{22}/k_{33} = 0.72$, obtained from (3.8) and the data (2.1). However, the fingerprint texture can be seen up to a value of $(P/d)_{\text{f}} = 0.98$ (see Figure 2). This contrast to the findings of press and Arrott may possibly be due to the different values of the elastic constant ratios.

From the point of view of applications to phase-change displays a few comments are appropriate. The voltage $V_{\text{ch,n}}$ is of great importance when one attempts to operate such displays in a multiplexing mode [7]. This is due to the finding that $V_{\text{ch,n}}$ is the only voltage at which a homogeneous as well as a fingerprint texture can be kept stable for long times without one of them growing at the expense of the other. The voltage V_G is important for the switching process from the homeotropic to the scroll texture, while the corresponding characteristic times τ_G determine the speed of this switching process. Furthermore when operating in a multiplexing mode one has to account for the time required to establish the scroll texture from the conical helix, since the latter may return directly to the homeotropic state when the voltage is raised too quickly back above V_G. For a fast switching to the homeotropic state the voltage V_1 is important, because for $V > V_1$ the fingerprint texture disappears speedily due to the generation of breaks in the cholesteric lines. The measurements of τ_h indicate the times associated with this switching process as a function of the applied voltage.

In applications utilizing the scroll texture, such as in some modes of operation of guest-host displays, it is important to know the limiting value of P/d above which the scroll texture appears directly after removal of the applied voltage. In this case too, small values of P/d may lead to after-images due to intermediate fingerprint-like textures generated by undulation [18].

We have confined this work to cells with homeotropic boundary conditions at the substrate and to one single nematic substance. The primary dependence considered was the one on the pitch-to-thickness ratio which can be varied most easily over an appreciable range of values. It is planned to extend these investigations to cells with homogeneous wall alignment. Also of interest are variations of the ratios of elastic constants and of the dielectric constants. However, these parameters cannot be easily varied independently and lead to more refined modifications of the effects considered.

Acknowledgements

The author has profited from valuable comments by Dr. C. von Planta and Dr. M. Schadt.

[1] G. H. Heilmeier and L. A. Zanoni, Appl. Phys. Lett. **13**, 91 (1968).
[2] D. L. White and G. N. Taylor, J. Appl. Phys. **45**, 4718 (1974).
[3] M. Schadt, J. Chem. Phys. **71**, 2336 (1979).
[4] P. G. De Gennes, Solid State Comm. **6**, 163 (1968).
[5] R. B. Meyer, Appl. Phys. Lett. **12**, 281 (1968).
[6] J. J. Wysocki, J. Adams, and W. Haas, Phys. Rev. Lett. **20**, 1024 (1968).
[7] K. H. Walter and H. H. Krüger, Ber. Bunsenges. **78**, 912 (1974).
[8] L. J. Yu and M. M. Labes, Mol. Cryst. Liq. Cryst. **28**, 423 (1974).
[9] M. J. Press and A. S. Arrott, J. de Phys. **37**, 387 (1976).
[10] M. J. Press and A. S. Arrott, Mol. Cryst. Liq. Cryst. **37**, 81 (1976).
[11] A. E. Stieb, J. de Phys. **41**, 961 (1980).
[12] S. K. Kwok and Liao York, J. Appl. Phys. **49**, 3970 (1978).
[13] M. Schadt and P. Gerber, to be published in Mol. Cryst. Liq. Cryst.

[14] C. J. Gerritsma and P. van Zanten, Phys. Lett. **37 A**, 47 (1971).
[15] M. Kawachi, O. Kogure, and Y. Kato, Japan. J. Appl. Phys. **13**, 1457 (1974).
[16] W. E. L. Haas and J. E. Adams, Appl. Phys. Lett. **25**, 263 (1974).
[17] W. Greubel, App. Phys. Lett. **25**, 5 (1974).
[18] A. Saupe and L. Yu, reported at the "Freiburger Arbeitstagung Flüssigkristalle", March 1980.
[19] E. Jakeman and E. P. Raynes, Phys. Lett. **39 A**, 69 (1972).
[20] P. E. Cladis and M. Kleman, Mol. Cryst. Liq. Cryst. **16**, 1 (1972).
[21] T. Akahane and T. Tako, Mol. Cryst. Liq. Cryst. **38**, 251 (1977).